Nov 5th, 12:00 AM - 12:00 AM

Cold-Formed Lean Duplex Stainless Steel Rectangular Hollow Sections in Combined Compression and Bending

Yuner Huang

Ben Young

Twenty-Second International Specialty Conference on Cold-Formed Steel Structures
St. Louis, Missouri, USA, November 5 & 6, 2014

Cold-formed Lean Duplex Stainless Steel Rectangular Hollow Sections in Combined Compression and Bending

Yuner Huang[1] and Ben Young[2]

Abstract

An experimental investigation of cold-formed lean duplex stainless steel members in combined compression and minor axis bending is performed. The test specimens were cold-rolled from flat strips of lean duplex stainless steel grade EN 1.4162 into two rectangular hollow sections. Different eccentricities were applied to the rectangular hollow sections, so that a beam-column interaction curve for each series of test can be obtained. Initial overall geometric imperfections of the members were measured prior to testing. The ultimate loads and the failure modes of each specimen were obtained. Failure modes include flexural buckling as well as interaction of local and flexural buckling were observed from the test specimens. The test strengths were compared with the design strengths predicted by the American, Australian/New Zealand and European specifications for stainless steel structures. It should be noted that these specifications do not cover the material of lean duplex stainless steel. Generally, the specifications are capable of predicting the beam-column strengths of the lean duplex stainless steel test specimens.

Introduction

Cold-formed lean duplex stainless steel, with both structural and economical advantages, is becoming an attractive choice as a construction material. It has a low nickel content compared to other grades of stainless steel, which reduced the material cost. In addition, it is regarded as a high strength material with the nominal yield strength (0.2% proof stress) of 450 MPa. However, investigation of such relatively new material is very limited. Huang and Young (2012) investigated the material properties of cold-formed lean duplex stainless steel, including the yield strength, ultimate strength, Young's modulus, residual stress, local imperfection, and stub column strengths. Huang and Young (2013, 2014a) as well as Theofanous and Gardner (2009) carried out experimental and numerical investigations on cold-formed lean duplex stainless steel columns. It

[1] Post-doctoral Fellow, Department of Civil Engineering, The University of Hong Kong, Pokfulam Road, Hong Kong, China

[2] Professor, Department of Civil Engineering, The University of Hong Kong, Pokfulam Road, Hong Kong, China

is found that the current design specifications generally provide conservative predictions to the column strengths of cold-formed lean duplex stainless steel. Modified column design rules based on the current design specifications have been proposed. Huang and Young (2014b) as well as Theofanous and Gardner (2010) investigated the structural behaviour of cold-formed lean duplex stainless steel flexural members. The flexural strengths of the structural members obtained from experimental and numerical investigations were compared with the design strengths predicted by different design rules. It is found that the existing design rules are generally conservative for the lean duplex stainless steel beams, and beam design rules were also proposed.

Structural members subjected to combined compression and bending are commonly used in construction. Previous researchers have investigated stainless steel structural members subjected to axial compression and bending. Kouhi et al. (2000) carried out tests on beam-column specimens of rectangular hollow section (RHS) for austenitic stainless steel grade EN 1.4301 (AISI 304). The test results were compared with the design strengths calculated by European Code. It is suggested that the limitation of the magnification factor should be ignored for a more conservative and less scattered predictions. Macdonald et al. (2007) conducted beam-column tests on lipped channel section for austenitic stainless steel grade EN 1.4301. It is found that interaction formula in European Code provides very conservative predictions for the beam-column strengths, when the virgin 0.2% proof stress and the linear elastic moment capacity were used. The predictions can be improved by using the 0.2% proof stress obtained from the fabricated sections, which include the strength enhancement due to cold-working, together with the moment capacity obtained from the beam tests. Greiner and Kettler (2008) evaluated the interaction factor in the interaction formulae for the prediction of beam-column strengths in EC3 (2005). Numerical simulations for I-sections and hollow sections of austenitic stainless steel (grade EN 1.4301) and duplex stainless steel (grade EN 1.4462) beam-column specimens were performed. A set of interaction factors for stainless steel beam-columns is proposed for different sections. It is found that the interaction formulae for carbon steel are also suitable for stainless steel, when the proposed interaction factors are used. Lui et al. (2012) conducted a series of tests on cold-formed duplex stainless steel grade EN 1.4462 (S32205). The beam-column test strengths were compared with design strengths predicted by the American Specification (ASCE) (2002) and Australian/New Zealand Standard (AS/NZS) (2001) for stainless steel. It is found that the current design specifications are generally conservative for the duplex stainless steel beam-columns. Talja and Salmi (1995) conducted beam-column tests for cold-formed RHS of austenitic stainless steel grade EN 1.4301. The test results were compared with the design strengths calculated by the beam-column design rules in the EC3 Part 1.3 (1993).

It is suggested that the limitation for magnification factor in the interaction formulae should not be used.

It should be noted that there is no investigation on cold-formed lean duplex stainless steel beam-column members up to now. The purpose of this paper is to provide test data on cold-formed lean duplex stainless steel rectangular hollow sections in combined axial compression and bending. Furthermore, the suitability of the current design rules in the American Specification (ASCE, 2002), Australian/New Zealand Standard (AS/NZS, 2001) and European Code (EC3, 2006) for cold-formed lean duplex stainless steel beam-columns is assessed. Lastly, the beam-column design rules were evaluated using reliability analysis.

Test specimens

Cold-formed lean duplex stainless steel members were tested under combined compression and bending in this study. The cold-formed lean duplex stainless steel grade EN 1.4162 is considered to be a high strength material with nominal 0.2% proof stress of 450 MPa (Yrjola, 2008). The test specimens were cold-rolled from flat strips into two rectangular hollow sections (RHS), with the nominal section sizes ($D\times B\times t$) of 100×50×2.5 and 150×50×2.5, where D, B and t are the depth, width and thickness of the cross-sections in millimeter, respectively. Each specimen was cut to a specified length of either 550 or 1550 mm. Both ends of the specimens were milled flat and then welded to 20 mm thick steel end plates for the specimens to be connected to the end bearings. Two different cross-sections with two different column lengths for each section provided four series of beam-column tests. The specimens were compressed by different eccentricities that ranged from around 2 to 55 mm, in order to obtain a beam-column interaction curve for each series of tests. A total of 18 beam-column specimens were tested in this study.

The test specimens were labeled such that the nominal cross-section geometry, specimen length, and loading eccentricities could be identified, as shown in Table 1. For example, the label “150×50×2.5L550E55” defines the following specimen: the dimension before the letter “L” indicates the nominal cross-section geometry ($D\times B\times t$) of the specimen; the letter “L” indicates the length of the specimen, and the following digits represent the nominal length of the specimen in millimeters (550 mm); the following part of the label “E55” indicates the nominal loading eccentricity at the ends of the specimen (55 mm). The measured loading eccentricities and cross-section dimensions of each test specimen are shown in Table 1.

Specimen	D (mm)	B (mm)	t (mm)	A (mm^2)	$e + \delta$ (mm)	δ/L
100×50×2.5L550E2	100.2	50.0	2.529	724.3	2.31	-1/1082
100×50×2.5L550E5	100.2	50.2	2.510	719.6	4.26	-1/2887
100×50×2.5L550E12.5	100.2	50.1	2.523	723.0	11.02	-1/4882
100×50×2.5L550E25	100.1	50.0	2.500	715.7	23.75	1/4068
100×50×2.5L550E55	100.2	50.1	2.555	731.8	54.19	1/3487
100×50×2.5L1550E5	100.2	50.0	2.530	724.4	4.78	1/4068
100×50×2.5L1550E12.5	100.2	50.0	2.526	723.3	11.32	-1/6102
100×50×2.5L1550E25	100.2	50.1	2.534	725.7	25.36	1/4882
100×50×2.5L1550E55	100.1	50.2	2.523	722.8	54.94	1/3015
150×50×2.5L550E5	150.1	49.8	2.457	942.2	4.53	1/1082
150×50×2.5L550E12.5	150.0	49.8	2.493	954.3	13.01	-1/2835
150×50×2.5L550E25	150.0	49.5	2.484	951.0	23.60	1/2165
150×50×2.5L550E55	150.0	49.8	2.519	967.7	55.25	-1/3543
150×50×2.5L1550E2	149.9	49.8	2.509	961.2	2.23	-1/8136
150×50×2.5L1550E5	150.0	49.6	2.490	953.5	4.55	-1/12205
150×50×2.5L1550E12.5	150.1	49.6	2.491	952.5	11.58	1/6102
150×50×2.5L1550E25	150.0	49.6	2.508	959.5	24.32	1/8136
150×50×2.5L1550E55	150.0	49.8	2.541	972.4	55.45	-1/4882

Table 1: Measured specimen dimensions and eccentricities as well as overall geometric imperfections at mid-length

The material properties of the test specimens were determined by tensile coupon tests on the flat portions of the cross-sections, as detailed in Huang and Young (2012). The tensile coupons were extracted from the same batch as the beam-column specimens in this study. The material properties obtained from the coupon tests, including the static 0.2% proof stress ($\sigma_{0.2}$), static tensile strength (σ_u), initial Young's modulus (E_o), elongation at fracture (ε_f) and Ramberg-Osgood parameter (n), are summarized in Table 2.

Section	$\sigma_{0.2}$ (MPa)	σ_u (MPa)	E_o (GPa)	ε_f (%)	n
100×50×2.5	625	727	200	49	6
150×50×2.5	664	788	202	35	4

Table 2: Measured material properties obtained from tensile coupon tests (Huang and Young, 2012)

Initial overall geometric imperfections of the beam-column specimens were measured prior to testing. Theodolite was used to obtain readings at the mid-length and near both ends of the specimens. The geometric imperfections were measured at the flat width near the corner, as shown in Fig. 1. The overall

geometric imperfections at mid-length (δ) are normalized by the specimen length (L), as summarized in Table 1. The positive value indicates that the overall geometric imperfection is away

The sign convention of the overall geometric imperfections and the location of measurement are shown in Fig. 1. The average absolute value of the overall geometric imperfections at mid-length were 1/2490, 1/4227, 1/1979, and 1/7179 of the specimen length for specimens in test Series 100×50×2.5L550, 100×50×2.5L1550, 150×50×2.5L550 and 150×50×2.5L1550, respectively. The maximum initial local geometric imperfections of the specimens measured by Huang and Young (2012) were 0.348 and 0.679 mm for cross-sections 100×50×2.5 and 150×50×2.5, respectively. These specimens were also from the same batch as the beam-column specimens in this study. The local geometric imperfection measurements are detailed in Huang and Young (2012).

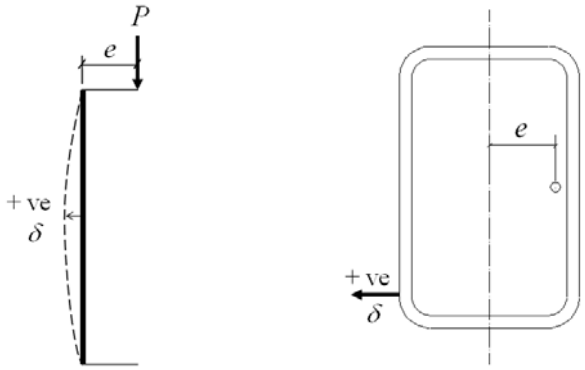

Figure 1: Sign convention and location of overall geometric imperfection measurements

Combined compression and bending tests

The cold-formed lean duplex stainless steel members were compressed between pinned ends with different eccentricities. A hydraulic testing machine was used to apply compressive force to the specimens. The test rig and the test setup are shown in Fig. 2. The specimens were welded with end plates. The pin-ended bearings were used at both upper and lower end supports to allow free rotation of the specimens about the minor axis only. Each pin-ended bearing is made up of knife-edge wedge plate and pit plate. The wedge plate has slot holes to allow adjustment of the column specimen to be loaded at a specified eccentricity. One of the pit plates was connected to a rigid plate at the upper end support, while

the other pit plate was connected to a special bearing at the lower end support. The end plates of the specimen were bolted to the two knife-edge wedge plates. The specimen was then put into the testing machine between the two pit plates, so that the knife-edge of the lower wedge plate was seated on the V-shape pit of the lower pit plate. Initially, the special bearing was free to rotate in any direction. The lower and upper wedges were positioned in-line and then applied approximately 5 kN to the specimen. This procedure would eliminate any possible gaps between the wedge plates and the pit plates in the pin-ended bearings, since the special bearing was free to rotate in any direction. The special bearing was then restrained from twisting and rotation by using the horizontal and vertical bolts, respectively. The applied load on the specimens was then released to approximately 2 kN to allow the test starts with a small initial load. The small compression load ensures full contact in the pin-ended bearings.

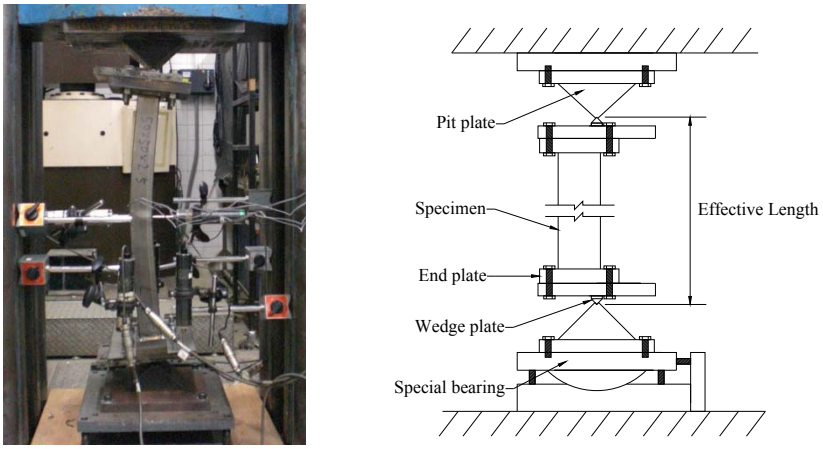

(a) Test rig (b) Setup

Figure 2: Schematic view of beam-column test

Three displacement transducers (LVDTs) were used to measure the axial shortening and the end rotation of the specimens. In addition, displacement transducers were located horizontally at mid-length of the specimens to measure the horizontal deflection of the specimen about the bending axis. Strain gauges were attached in the axial direction at mid-length of the specimens to determine the loading eccentricity and local buckling. Four strain gauges were located on the webs near the corners for all specimens to determine the loading eccentricity. Two additional strain gauges were located in the middle of the webs for columns having specimen length of 550mm to observe the occurrence of local buckling.

Displacement control was used to drive the hydraulic actuator at a constant speed of 0.2 mm/min for all tests. The static load was recorded by pausing the applied straining for 2 min near the ultimate load and post-ultimate load. A data acquisition system was used to record the applied load, the readings of the LVDTs and strain gauges at regular intervals during the tests.

It is important to measure the eccentricity (e) accurately, in order to compare the test strengths directly with the design strengths calculated from the measured loading eccentricity. Prior to the tests, the distance between the minor axis of the specimens and the knife edge of the wedge plate was adjusted to a specified eccentricity. Four strain gauges and a displacement transducer were used to determine the loading eccentricity at the mid-length of the specimens during testing. The applied load, longitudinal strains and overall deflection at mid-length about the bending axis of the specimens were recorded to determine the loading eccentricity. The bending moment of the specimens at mid-length equals to $E_o I_y \kappa$, and also equals to the applied compressive load (P) multiply by the loading eccentricity ($e + \delta$) together with the lateral deflection (Δ). Therefore, the measured loading eccentricity is determined as ($e + \delta$) = ($E_o I_y \kappa / P - \Delta$), where E_o = initial Young's modulus; I_y = second moment area of the sections about the minor axis; κ = curvature of the specimens which was calculated using the readings of the strain gauges; P = applied compressive load; and Δ = overall horizontal deflection at mid-length of the specimens about the bending axis. The measured loading eccentricity was obtained for each specimen during the initial stage of loading in the elastic range of the tests, as shown in Table 1.

The experimental ultimate axial loads (P_{Exp}), end moments ($M_{end,Exp}$), second-order elastic moments ($M_{e,Exp}$) and inelastic moments ($M_{i,Exp}$) corresponding to ultimate axial loads, and the failure modes of the beam-column tests are shown in Table 3, where Δ_u is the overall horizontal deflection at mid-length of the specimen at ultimate axial load and P_e is the elastic buckling load. The curves of the axial load (P) versus the inelastic moment as well as the axial load versus the end moment for Series 100×50×2.5L550 is shown in Fig 3. The points corresponding to the ultimate axial load (P_{Exp}) on the axial load versus inelastic moment curves are also indicated by the symbol circles, as shown in Fig 3. The failure modes observed at ultimate load of the specimens involved flexural buckling (F) and interaction of local and flexural buckling (L+F), as shown in Table 3.

Specimen	Failure mode	P_{Exp} (kN)	$M_{end,Exp}$ (kNmm)	$M_{i,Exp}$ (kNmm)	$M_{e,Exp}$ (kNmm)
100×50×2.5L550E2	L+F	325.7	752.4	1707.6	973.8
100×50×2.5L550E5	L+F	294.7	1255.4	2377.2	1581.3
100×50×2.5L550E12.5	L+F	226.5	2496.0	3765.0	2963.8
100×50×2.5L550E25	L+F	173.3	4115.9	5066.4	4688.8
100×50×2.5L550E55	L+F	99.9	5413.6	6149.1	5813.6
100×50×2.5L1550E5	F	151.2	722.7	4455.5	2181.9
100×50×2.5L1550E12.5	F	127.8	1446.7	5260.4	3332.1
100×50×2.5L1550E25	F	97.8	2480.2	6199.7	4352.3
100×50×2.5L1550E55	F	70.0	3845.8	6772.5	5558.9
150×50×2.5L550E5	L+F	290.8	1317.3	2446.9	1542.4
150×50×2.5L550E12.5	L+F	217.7	2832.3	3869.4	3175.6
150×50×2.5L550E25	L+F	173.9	4104.0	5178.1	4496.5
150×50×2.5L550E55	L+F	105.4	5823.4	6568.7	6138.6
150×50×2.5L1550E2	L+F	218.6	487.5	2654.4	1531.6
150×50×2.5L1550E5	L+F	188.5	857.7	3275.3	2127.7
150×50×2.5L1550E12.5	L+F	149.3	1728.9	4022.0	3290.6
150×50×2.5L1550E25	L+F	114.3	2779.8	5776.3	4347.6
150×50×2.5L1550E55	L+F	75.3	4175.4	6559.3	5443.3

Note: $M_{end,Exp} = P_{Exp}(e+\delta)$; $M_{i,Exp} = P_{Exp}(e+\delta+\Delta_u)$; $M_{e,Exp} = M_{end,Exp}/(1-P_{Exp}/P_e)$

Table 3: Experimental results

Reliability analysis

The reliability of the beam-column design rules in the current specifications, including ASCE (2002), AS/NZS (2001) and EC3 (2006), was evaluated using reliability analysis. It should be noted that the design rules in the European Codes are calibrated according to the guidelines given in Eurocode 0 (EC0, 2005), in which a different method of reliability analysis is described compared with the method in the ASCE Specification. However, for the purpose of direct comparison, the reliability analysis of ASCE is used for European Code in this study. Reliability analysis is detailed in the Commentary of the ASCE Specification (2002). A target reliability index of 2.5 for stainless steel structural members is used as a lower limit in this study. The design rules are considered to be reliable if the reliability index (β_0) is greater than or equal to 2.5. The resistance factors (ϕ_0) of 0.85, 0.90 and 1.00 for the design axial strength, and 0.90, 0.90 and 1.00 for design flexural strength as recommended by the ASCE (2002), AS/NZS (2001) and EC3 (2006) specifications, respectively, were used in the reliability analysis. The load combinations of 1.2DL+1.6LL, 1.25DL+1.5LL and 1.35DL+1.5LL were used in the reliability analysis for

ASCE (2002), AS/NZS (2001) and EC3 (2006), respectively, where DL is the dead load and LL is the live load. The Eq. 6.2-2 in the ASCE Specification was used in calculating the reliability index. The statistical parameters M_m = 1.10, F_m = 1.00, V_M = 0.10 and V_F = 0.05, which are the mean values and coefficients of variation for material properties and fabrication factors for compression members and flexural members, in the commentary of the ASCE Specification were adopted. The mean value (P_m) and coefficient of variation (V_P) of the tested-to-predicted load and moment ratios are shown in Table 4. In calculating the reliability index, the correction factor Eq. F1.1-4 in the North American Specification for the design of cold-formed steel structural members AISI S100 (2012) was used to account for the influence due to a small number of tests.

Design rules and comparison with beam-column strengths

The *unfactored* design strengths (nominal strengths) for members subjected to combined compression and bending were calculated using the American Specification (ASCE, 2002), Australian/New Zealand Standard (AS/NZS, 2001), and European Code (EC3, 2006). The design strengths were calculated using the average measured cross-section dimensions and the measured material properties for each specimen as detailed in Tables 1-2. The design rules provided in these three specifications for stainless steel members under combined axial load and bending for RHS are described in this Section. It should be noted that these specifications do not cover the material of lean duplex stainless steel. Therefore, the current beam-column design rules for lean duplex stainless steel are assessed in this study. The test strengths are compared with the *unfactored* design strengths (nominal strengths) for the combined compression and bending tests as shown in Table 4. The beam-column interaction curves of Series 100×50×2.5L550 are plotted, as shown in Figure 3. The available column strengths (Huang and Young, 2013) and flexural members (Huang and Young, 2014b) of sections 100×50×2.5 and 150×50×2.5 are also used in the comparison, in order to investigate the full range of beam-column interaction curves. Hence, a total of 22 column strengths and 26 flexural strengths are compared.

For the American Specification, the unfactored beam-column strengths (nominal strengths) subjected to axial compression and minor axis are calculated by Eqs. (1) – (3) in this study,

$$P_u/P_n + C_m M_{e,u}/M_n \leq 1.0 \quad (1)$$

$$P_u/P_{no} + M_{end,u}/M_u \leq 1.0 \quad (2)$$

$$P_u/P_n + M_{end,u}/M_n \leq 1.0 \text{ (when } P_u/P_n \leq 0.15) \quad (3)$$

where P_u is the design axial compressive strength; $M_{e,u}$ is the design second-order elastic moment, which is calculated by $M_{e,u} = M_{end,u}/(1-P_u/P_e)$; $M_{end,u}$ is the design end moment, which is calculated by the design axial compressive strength (P_u) multiplying by loading eccentricity ($e + \delta$); C_m is a coefficient and taken as 1.0 in this study; P_n and M_n are the nominal axial strength and flexural strength calculated by the design rules for columns and beams in the ASCE (2002), respectively; P_{no} is the nominal axial strength taken the buckling stress as the yield stress in the ASCE (2002). Iterative procedure is required to calculate both P_n and M_n. It is shown in Table 4 that the mean values of P_{Exp}/P_{ASCE} and $M_{e,Exp}/M_{ASCE}$ ratios are equal to 1.06 and 1.13, with the corresponding values of COV equal to 0.058 and 0.116, respectively. The reliability index (β_0) of P_{Exp}/P_{ASCE} and $M_{e,Exp}/M_{ASCE}$ are greater than the target value of 2.5. Therefore, the ASCE specification provides accurate and reliable prediction for lean duplex stainless steel beam-columns. However, the calculation involves tedious iterative procedure.

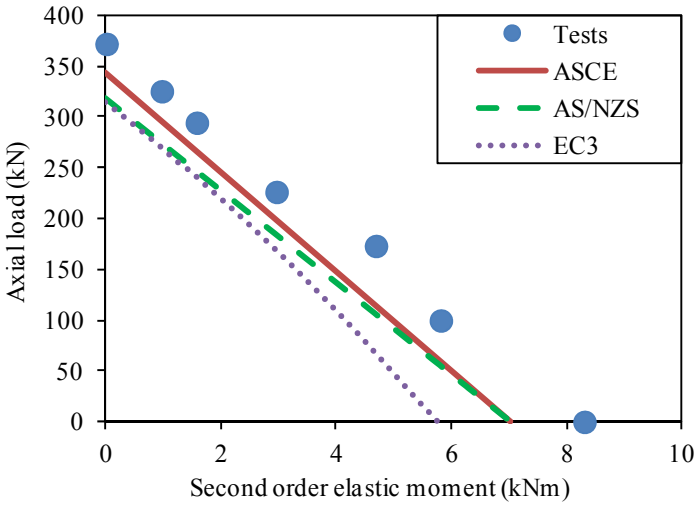

Figure 3: Interaction curve of Series 100×50×2.5L550

For the Australian/New Zealand Standard, the beam-column design rules in are identical to those in the ASCE Specification (2002), except that the nominal axial strength (P_n) and flexural strength (M_n) are calculated in accordance with the design rules for columns and beams in the AS/NZS (2001), respectively. The explicit method (alternative method) in Section 3.4.2 of the AS/NZS Standard (2001) was used in calculating the nominal axial strength (P_n) in this study. The design axial compressive strength (P_u) and design second-order elastic moment

($M_{e,u}$) in the AS/NZS (2001) are represented by $P_{AS/NZS}$ and $M_{AS/NZS}$, respectively, as shown in Table 4. It is shown that the AS/NZS Standard is generally conservative for the lean duplex stainless steel beam-columns. The mean values of $P_{Exp}/P_{AS/NZS}$ and $M_{e,Exp}/M_{AS/NZS}$ ratios equal to 1.13 and 1.26, with the corresponding values of COV equal to 0.046 and 0.172, respectively. The reliability indices (β_0) of $P_{Exp}/P_{AS/NZS}$ and $M_{e,Exp}/M_{AS/NZS}$ are 2.84 and 2.66, respectively, which are greater than the target values.

For the European Code, the strengths for members subjected to axial compression and minor axis bending is shown in Eq. (4), according to clause 5.5 of the EC3 Part 1.4 (2006),

$$P_u / P_n + k_z [(M_{end,u} + P_u \times e_N) / (\beta_W \times W_{pl} \times f_y)] \leq 1.0 \qquad (4)$$

where P_u is the design axial compressive strength; $M_{end,u}$ is the design end moment, which is calculated as the design axial compressive strength (P_u) multiplying by loading eccentricity ($e + \delta$); P_n is the nominal axial strength calculated by the design rules for columns in the EC3 (2006); e_N is the shifts in the neutral axes when the cross-section is subject to uniform compression, which is taken as zero for the RHS and SHS in this study. β_W is the coefficient, W_{pl} is the plastic modulus of full cross-section, f_y is the yield stress, and k_z is the interaction factor. Section classification of the specimens is required to calculate the design strengths. The design axial compressive strength (P_u) calculated using Eq. (4) is represented by P_{EC3} in this study, as shown in Table 4. Unlike the ASCE Specification (2002) and AS/NZS Standard (2001), the EC3 (2006) does not require the multiplication of $1/(1-P_u/P_e)$ in the calculation of design strengths in Eq. (4). For comparison purposes, the design second-order elastic moment (M_{EC3}) is calculated by the end moment ($M_{end,u}$) multiplied by $1/(1-P_u/P_e)$. Hence, $M_{EC3} = M_{end,u}/(1-P_u/P_e)$, as shown in Table 4. It is shown that the design rules in EC3 (2006) are quite conservative the cold-formed lean duplex stainless steel beam-column specimens in this study. The mean values of P_{Exp}/P_{EC3} and $M_{e,Exp}/M_{EC3}$ ratios equal to 1.16 and 1.34 with the corresponding values of COV equal to 0.090 and 0.274, respectively. The reliability index (β_0) of P_{Exp}/P_{EC3} and $M_{e,Exp}/M_{EC3}$ are 2.42 and 2.04, respectively. Generally speaking, the EC3 (2006) provides the most conservative and scattered predictions. The interaction factor (k_z) affected the shape of the interaction curves. The conservative predictions of the beam-column strengths were mainly contributed by the conservative predictions of the axial strengths and flexural strengths in the EC3.

	$\frac{P_{Exp}}{P_{ASCE}}$	$\frac{P_{Exp}}{P_{AS/NZS}}$	$\frac{P_{Exp}}{P_{EC3}}$	$\frac{M_{e,Exp}}{M_{ASCE}}$	$\frac{M_{e,Exp}}{M_{AS/NZS}}$	$\frac{M_{e,Exp}}{M_{EC3}}$
Number of tests	22	22	22	26	26	26
Mean (P_m)	1.06	1.13	1.16	1.13	1.26	1.34
COV(V_P)	0.058	0.046	0.090	0.116	0.172	0.274
Resistance factor (ϕ_0)	0.85	0.90	1.00	0.90	0.90	1.00
Reliability index (β_0)	3.00	2.84	2.42	2.76	2.66	2.04

Table 4: Comparison of test strengths with design strengths for all beam-column specimens

Conclusions

A test program on cold-formed lean duplex stainless steel beam-columns is presented. The members were subjected to combined compression and minor axis bending. Four series of test specimens with two rectangular cross-sections and two member lengths were compressed at various eccentricities. The ultimate loads and failure modes of each specimen were obtained. The test strengths were compared with the design strengths calculated by the American, Australian/New Zealand and European specifications. It should be noted that these three specifications do not cover the material of lean duplex stainless steel, and thus their applicability in designing lean duplex stainless steel beam-columns was assessed. Generally, the current design specifications are conservative and reliable in predicting the beam-column strengths of cold-formed lean duplex stainless steel in this study. It is shown that the American Specification provides accurate and reliable predictions for lean duplex stainless steel beam-columns, but iterative procedure is required in the calculation. European Code generally provides quite conservative predictions for the beam-column specimens compared to the American Specification and Australian/New Zealand Standard predictions.

Appendix. – References

AISI S100. (2012). North American Specification for the design of cold-formed steel structural members. AISI S100-2012, North American Cold-formed Steel Specification. American Iron and Steel Institute, Washington D.C., USA.

ASCE (2002). Specification for the design of cold-formed stainless steel structural members. SEI/ASCE 8-02; Reston, VA: American Society of Civil Engineers.

AS/NZS (2001). Cold-formed stainless steel structures. Australian/New Zealand Standard, AS/NZS 4673:2001. Sydney (Australia): Standards Australia.

EC0. (2005). Eurocode – Basis of structural design. EN 1990:2002+A1:2005. CEN. European Committee for Standardization, Brussels.

EC3 (1993). Design of steel structures, Part 1.3: Cold formed thin gauge members and sheeting. European Committee for Standardization (document CEN/TC250/SC3: N269E), ENV 1993-1-3 (Draft), Brussels.

EC3 (2005). Design of steel structures – Part 1-4: General rules— Supplementary rules for stainless steel. European Committee for Standardization, EN 1993-1–4, Brussels.

EC3 (2006). Design of steel structures – Part 1.4: General rules – Supplementary rules for stainless steels. European Committee for Standardization, ENV 1993-1-4, CEN, Brussels.

Greiner R, Kettler M. (2008). "Interaction of bending and axial compression of stainless steel members." *Journal of Constructional Steel Research*; 64(11): 1217-24.

Huang Y, Young B. (2012). "Material properties of cold-formed lean duplex stainless steel sections." *Thin-walled Structures*; 54: 72-81.

Huang Y, Young B. (2013). "Tests of pin-ended cold-formed lean duplex stainless steel columns." *Journal of Constructional Steel Research*; 82: 203-215.

Huang Y, Young B. (2014a). "Structural performance of cold-formed lean duplex stainless steel columns." *Thin-Walled Structures*. (In press)

Huang Y, Young B. (2014b). "Experimental and numerical investigation of cold-formed lean duplex stainless steel flexural members." *Thin-Walled Structures*; 73: 216 – 228.

Kouhi J, Talja A, Salmi P, Ala-Outinen T. (2000). "Current R&D work on the use of stainless steel in construction in Finland." *Journal of Constructional Steel Research*; 54(1): 31-50.

Lui WM, Young B, Ashrah M. (2012). "Eccentric compression tests on high strength duplex stainless steel columns." *Proceeding of 14th International Symposium on Tubular Structures*.

Macdonald M, Rhodes J, Kotelko M. (2007). "Stainless steel stub columns subject to combined bending and axial loading." *Thin-walled Structures*; 45(10-11): 893-897.

Talja A, Salmi P. (1995). "Design of stainless steel RHS beams, columns and beam-columns." VTT Building Technology, Finland.

Theofanous M, Gardner L. (2009). "Testing and numerical modelling of lean duplex stainless steel hollow section columns." *Journal of Engineering Structures*; 31(12): 3047-3058.

Theofanous M, Gardner L. (2010). "Experimental and numerical studies of lean duplex stainless steel beams." *Journal of Constructional Steel Research*; 66(6): 816-25.

Yrjola P. (2008). Stainless steel hollow sections handbook. Finnish Constructional Steelwork Association, Finland.

Appendix. – Notation

A	full area
B	overall width of specimen
C_m	coefficient in American Specification and Australian/New Zealand Standard
COV	coefficient of variation
D	overall depth of specimen
E_o	initial Young's modulus
e	eccentricity
e_N	shift in the neutral axes for cross-section subjected to uniform compression
F_m	mean value of fabrication factor
f_y	yield stress
I_y	second moment area about the minor axis
k_z	interaction factor
L	specimen length
M_{ASCE}	unfactored design second-order elastic moment of beam-column for American Specification
$M_{AS/NZS}$	unfactored design second-order elastic moment of beam-column for Australian/New Zealand Standard
M_{EC3}	unfactored design second-order elastic moment of beam-column for European Code

$M_{e,Exp}$	experimental second-order elastic moment corresponding to ultimate load
$M_{e,u}$	design second-order elastic moment corresponding to ultimate load
$M_{end,Exp}$	experimental end moment corresponding to ultimate load
$M_{end,u}$	design end moment corresponding to ultimate load
$M_{i,Exp}$	experimental inelastic moment corresponding to ultimate load
M_m	mean value of material factor
M_n	nominal flexural strength
M_u	design flexural strength
n	Ramberg-Osgood parameter
P	applied compression load
P_e	elastic buckling load
P_{ASCE}	unfactored design axial load of beam-column for American Specification
$P_{AS/NZS}$	unfactored design axial load of beam-column for Australian/New Zealand Standard
P_{EC3}	unfactored design axial load of beam-column for European Code
P_{Exp}	experimental ultimate axial load
P_m	mean value of tested-to-predicted load ratio
P_n	nominal strength of compressive member
P_{no}	nominal strength of compressive member calculated by the American Specification with the buckling stress taken as yield stress
P_u	design axial compressive strength
t	thickness of specimen
V_F	coefficient of variation of fabrication factor
V_M	coefficient of variation of material factor
V_p	coefficient of variation of tested-to-predicted load ratio
W_{pl}	plastic modulus
β_W	coefficient
β_0	reliability index
Δ	overall horizontal deflection at mid-length
Δ_u	overall horizontal deflection at mid-length corresponding to the ultimate axial load
δ	initial overall imperfection of column
ε_f	tensile strain after fracture based on gauge length of 25 mm
ϕ_0	resistance factor
κ	curvature
σ_u	static tensile strength
$\sigma_{0.2}$	static 0.2% tensile proof stress (yield stress).